Hindawi
Advances in Civil Engineering
Volume 2019, Article ID 9871424, 11 pages
https://doi.org/10.1155/2019/9871424

Research Article

Energy Evolution and Mechanical Features of Granite Subjected to Triaxial Loading-Unloading Cycles

Feng Pei,[1,2] **Hongguang Ji**,[1,2] **and Tongzhao Zhang**[1,2]

[1]*School of Civil and Resource Engineering, University of Science and Technology Beijing, Beijing 100083, China*
[2]*Beijing Key Laboratory of Urban Underground Space Engineering, University of Science and Technology Beijing, Beijing 100083, China*

Correspondence should be addressed to Feng Pei; ustbpeifeng@163.com

Received 12 September 2018; Accepted 16 December 2018; Published 6 January 2019

Guest Editor: Jian Sun

Energy evolution varies during the whole process of rock deformation, and mechanical parameters are markedly altered under cyclic loading and unloading. In order to investigate the effects of confining pressure on energy evolution and mechanical parameters, cyclic loading and unloading experiments were performed for granite under six different confining pressures. The experiment revealed the confining pressure effect on variation and allocation pattern of energy and mechanical characteristics. Four characteristic energy parameters, namely, storage energy rock, storage energy limit, energy storage ratio, and energy dissipation ratio, were proposed to describe energy storage and dissipation properties of rock. Elastic modulus and dissipation ratio presented a downward "U" and "U"-shaped trends, respectively, with loading and unloading cycles, while Poisson's ratio increased linearly at the same time. Elastic energy was accumulated mainly before peak stress, while the energy dissipation and release were dominant after the peak strength. As the confining pressure increased, efficiency of energy accumulation and storage limit improved. An exponential function was proposed to express the relationship between the energy storage limit and confining pressure. Dissipation energy increased nonlinearly with the strain, and the volume dilatancy point defined the turning point from a relatively slow growth to an accelerated growth of dissipation energy. The dilatancy point can be used as an important indication for the rapid development of dissipation energy.

1. Introduction

Many engineering projects have shown that rock is not in a stable stress environment but is subjected to a cyclic loading-unloading stress environment. Deformation and failure of granite under engineering disturbance is a very complicated damage evolution process, and failure is governed by energy storing and dissipation phenomenon [1]. Rock is in a dynamic evolution process of input energy, accumulation energy, dissipation energy, and release energy. The proportion of energy allocation is dependent on the stress level and determines failure modes of rock. Demand for underground space and resources from the deep is becoming increasingly intense with the depletion of shallow mineral resources and the improvement of science and technology. Consequently, rock burst and other dynamic disasters occur frequently, particularly in China. Accumulation of energy and rapid release are the key control factors of rock burst [2–6]. Therefore, it is imperative to study the dynamic disasters such as rock burst from the aspect of energy.

The influence of loading and unloading cycles on energy variation and mechanical properties has been studied by domestic and foreign researchers. Wang et al. [7] studied the characteristics of energy transformation of total energy, elastic strain energy, and dissipation energy and revealed the energy damage evolution mechanism of the jointed rock mass. Rock damage from the perspective of energy was defined by Peng et al. [8]. Zhang and Gao [9, 10] revealed the trends of evolution of elastic energy and dissipation energy under different confining pressures and analysed the nonlinear relationship of different energy conversion mechanisms. Energy dissipation and release of rocks under different stress paths were summarized by Cheng et al. [11]. Bagde and Petroš [12] revealed that fatigue and dynamic

energy behaviour of rock subjected to cyclic loading. Deng et al. [13, 14] have investigated the relationship among energy evolution, residual strain, and damage variable parameters. The relationships between strain energy and strain under three confining pressures were fitted by Tian and Yu [15], and the concept of crack development coefficient was proposed. The above research work has greatly promoted the development of rock energy theory.

However, at present, the energy characteristics under the special loading level such as peak stress are paid more attention, while the real-time evolution and distribution of energy throughout the whole process of failure are insufficiently studied in the process of research. The purpose of this paper is to perform laboratory tests to explore quantitative relationships between energy and mechanical parameters throughout the whole process of failure. The results are expected to provide reference for rock mechanics tests and dynamic disaster prediction.

2. Rock Samples and Experimental Methods

2.1. Rock Samples. All rock samples used in the tests were granite from a depth of −1243~−1245 m and were collected from the geological borehole of the new main shaft in Xincheng gold mine, Shandong province. Rocks are medium-fine grain structure. The analysis of a series of rock slices by optical microscopy shows that the main minerals are as follows: quartz, plagioclase, alkaline feldspar, and biotite. According to the QAP classification method, it can be named porphyritic granodiorite. Rock samples were processed into cylinders of 50 mm × 100 mm, according to the ISRM method recommended by international rock mechanics testing. A NM-4B ultrasonic testing instrument was used to detect wave velocity of samples. In order to avoid testing error caused by the variability of samples, samples with similar wave velocity were selected for triaxial testing. Basic physical parameters of rock samples are shown in Table 1.

Table 1: Basic physical parameters of rock samples.

Number	Diameter (mm)	Height (mm)	Wave velocity ($m \cdot s^{-1}$)	Density ($kg \cdot m^{-3}$)
X-H-1	50.01	100.03	4034	2676
X-H-2	49.97	99.99	4004	2689
X-H-3	49.98	99.99	4100	2685
X-H-4	50.00	100.00	4012	2683
X-H-5	50.01	100.01	3988	2695
X-H-6	49.98	100.02	4029	2658

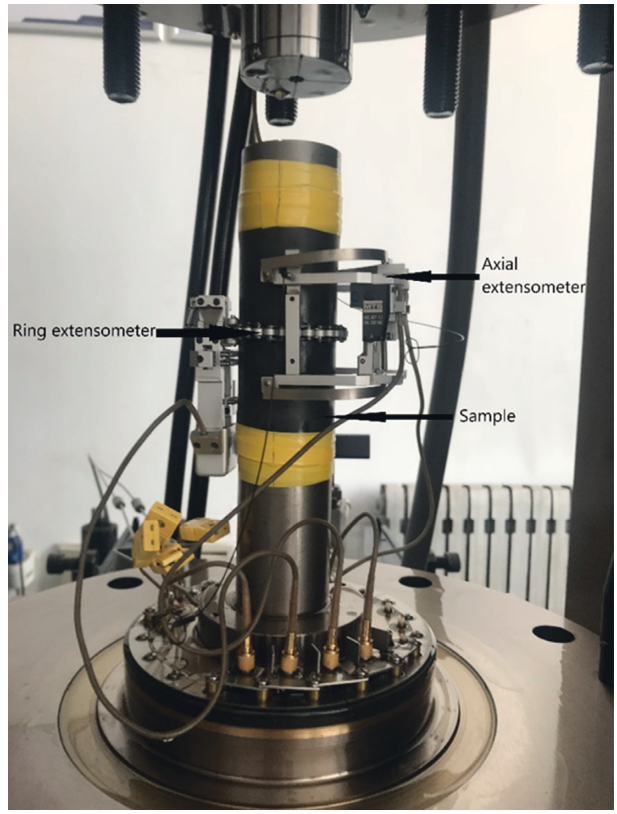

Figure 1: Sample installation.

2.2. Experimental Methods. A series of cyclic loading and unloading tests were conducted by an MTS815 rock mechanics testing machine. The maximum axial loading of the testing machine is 2700 kN, and the maximum confining pressure can be applied to 140 MPa. Axial and circumferential extensometers were used to measure axial and circumferential deformations in real time by placing extensometers in the middle of rock samples, as shown in Figure 1. The maximum ranges of axial and circumferential extensometers are 5 mm and 8 mm, respectively. To simulate the energy evolution in rock at different depths below ground, confining pressures of 1, 10, 20, 30, 40, and 45 MPa were applied in the laboratory tests. 2 kN axial pressure was applied firstly to properly hold the specimens in the testing machine, and then, confining pressure was applied to the predetermined value. Axial pressure was applied according to the circumferential deformation. The loading rate was 0.02 mm/min, and the unloading rate was 0.04 mm/min. In the next loading cycle, the peak loading was increased by 40–60 kN compared to the previous cycle. The loading-unloading path was as follows: 0 kN ⟶ 200 kN⟶5 kN ⟶ 260 kN ⟶ 5 kN ⟶⋯⟶ destruction, as shown in Figure 2.

3. Results and Analysis

3.1. Stress-Strain Curves and Failure Modes. Stress-strain curves under 45 MPa confining pressure and failure modes under different confining pressures are shown in Figure 3. The mechanical parameters of these rocks are shown in Table 2.

(1) The outer envelopes of cyclic loading and unloading under different confining pressures are similar to conventional loading, and samples have undergone four distinct stages: compaction stage, elastic deformation stage, unsteady fracture development stage, and postpeak failure stage. Due to the closure

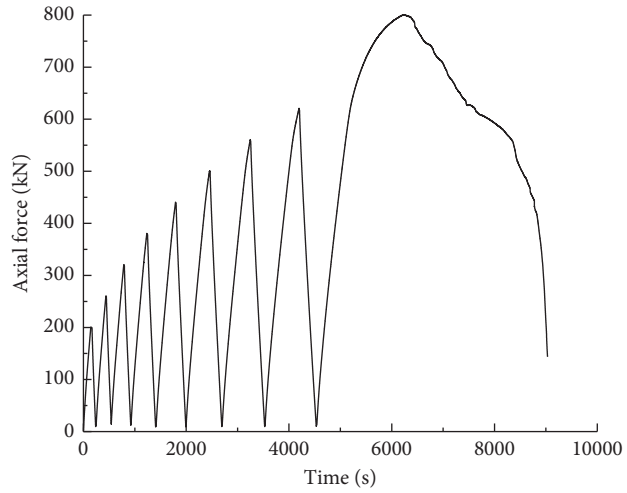

Figure 2: X-H-3 cyclic loading-unloading path.

of initial cracks caused by high confining pressure, the compaction stage was not obvious for larger confining pressure. The peak strength and peak strain were improved significantly with the larger confining pressures. Large confining pressure increased crack initiation stress and limited the development of circumferential deformation. Strength and rigidity were enhanced at the same time and had obvious confining pressure effect.

(2) Under 1 MPa and 10 MPa confining pressures, the local region failed and small pieces fell off from the surface, and there were many small fragments beside the main crack, indicating local tensile failure. Under 20 MPa and 30 MPa confining pressures, small-scale failure existed on the surface of rock mass, and shear failure was the main failure mode. Under 40 MPa and 45 MPa confining pressures, rock samples were divided into two blocks separated by the main crack. Failure occurred with almost no surface fracture and accompanied by loud noise. With an increase in confining pressure, the number of surface fractures gradually decreased and failure modes changed from tension and shear coexistence to shear failure. Larger confining pressure restrained the development of surface cracks, and energy consumption was insufficient, so it was easy to produce through fracture surface. Sudden release of large amount of elastic energy was the intrinsic driving force for rock failure, and the failure mode was closely related to the characteristics of an internal structure.

3.2. Nonlinear Transformation of Energy. Elastic energy is mainly stored in rock mass in the form of elastic strain, and it is reversible. Dissipation energy includes plastic deformation energy, surface damage energy, thermal energy, and radiation energy, and it is irreversible. The energy released after unloading is the elastic energy accumulated at a certain stress level. The decrease value relative to the total energy is the dissipation energy at this stress level. It is unrealistic to monitor each energy in real time during the dynamic loading. The energy evolution is mainly manifested by the dynamic balance of input energy, elastic strain energy, and dissipation energy [16] as follows:

$$\begin{aligned} u_{i\mathrm{e}} &= \int_{\varepsilon}^{\varepsilon'} \sigma_i d\varepsilon_i, \\ u_{i\mathrm{d}} &= \int_{0}^{\varepsilon'} \sigma_i d\varepsilon_i - \int_{\varepsilon''}^{\varepsilon'} \sigma_i d\varepsilon_i, \\ u &= u_{\mathrm{e}} + u_{\mathrm{d}}, \end{aligned} \tag{1}$$

where u is the total energy obtaining from the testing machine, u_{e} is the elastic strain energy, and u_{d} is the dissipation energy. ε' is the unloading strain, σ'' is the unloading stress, and ε'' is the residual strain.

Different forms of energy differ not only in quantity but also in quality. Elastic energy belonging to high-quality energy can be converted into other forms of energy. Surface fracture energy, radiation energy, and thermal energy are low-quality energy. The energy evolution processing of rock under loading is shown in Figure 4. Strain hardening and strain softening mechanisms are involved in the whole loading process. The strain hardening mechanism is that energy of samples is stored in the rock in the form of elastic strain energy. At the microscopic level, strain hardening is the interaction between rock particles and change of the contact mode between grain boundaries. The strain softening mechanism is characterized by low-quality energy such as plastic deformation energy, thermal energy, damage energy, and radiation energy and is featured by microscopic crack propagation, grain slip, and intergranular and transgranular failure. The two strain mechanisms coexist in the whole loading process, and they are mutually restricted and mutually promoted. In addition, energy absorption and consumption also have obvious zoning characteristics; an increase in energy in one region will restrict the energy development in other regions.

The relationship between internal structure and energy development is shown in Figure 5. Strain hardening played a dominant role before unsteady crack propagation, and input energy was mainly converted into elastic strain energy. Stiffness restrained the development of strain softening mechanism. Elastic strain energy gradually reached its limit and tended to be in the saturation state with the development of strain hardening mechanism, and strain softening mechanism beginning to strengthen immediately. Higher stress levels accelerated damage and deformation in internal structure. When the input energy exceeded energy storage limit, the energy stored in the rock would be released rapidly. Readjusted internal structure reduced energy storage limit, and the strain softening mechanism was strengthened at the same time after peak stress.

The ratio of elastic strain energy to energy storage limit under current stress is defined as the rock energy level. The variation in the rock energy level with stress is shown in Figure 6. Relatively less energy was stored in rock in the initial loading stage. Producing a large amount of elastic energy led to increase in the energy level in the elastic stage. The highest energy level occurred at peak stress, and even a

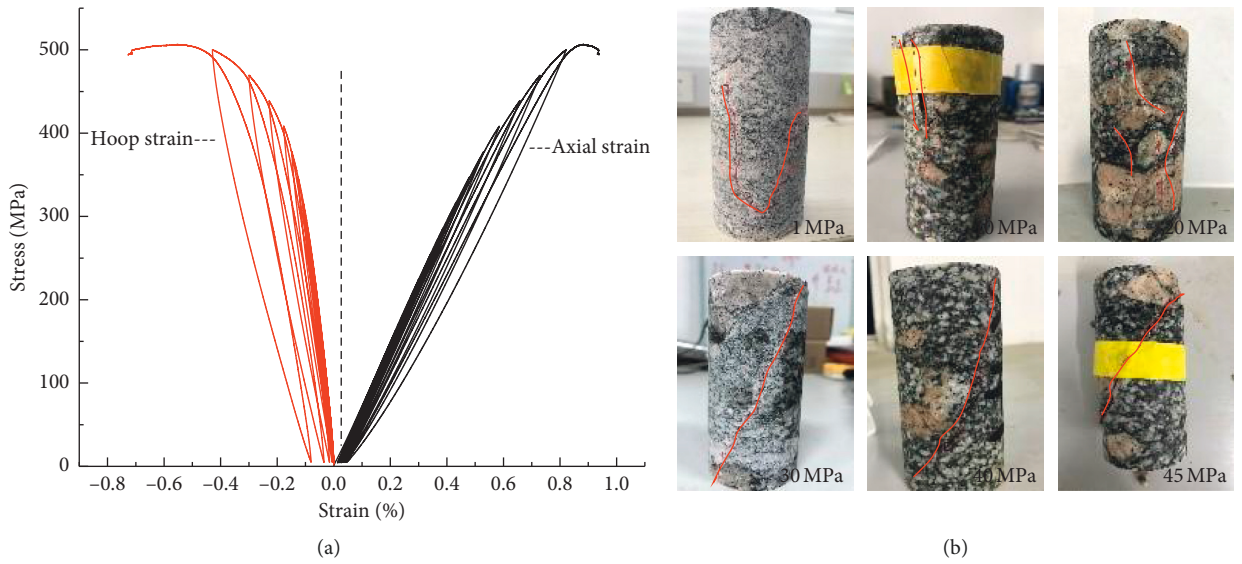

Figure 3: (a) Stress-strain curves and (b) failure modes.

Table 2: Mechanical parameters of samples.

Confining pressure (MPa)	Dilatancy stress (MPa)	Peak stress (MPa)	Stress level (%)	Axial strain (%)	Hoop strain (%)
1	158.11	204.07	0.77	0.40	0.21
10	219.52	295.13	0.74	0.50	0.30
20	234.82	343.21	0.68	0.55	0.37
30	285.15	380.15	0.75	0.69	0.41
40	337.01	408.32	0.83	0.78	0.49
45	389.00	506.39	0.77	0.83	0.54

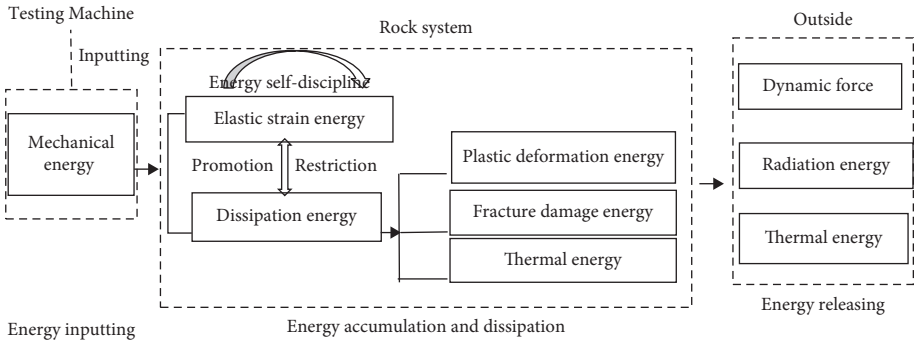

Figure 4: Energy conversion relationship.

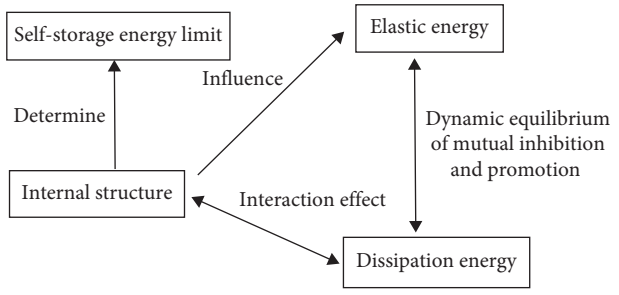

Figure 5: Interaction between internal structure and energy.

small increment in input energy may cause sharp energy release. These results suggested that the energy level represented the risk coefficient; the high risk coefficient bring about more severe damage under external disturbance.

3.3. Development of Energy Density and Its Allocation. Storing energy through deformation from testing machines is an inherent property of hard rocks such as granite, which is defined as storage energy rock. Furthermore, the elastic strain energy stored at peak strength is defined as the energy

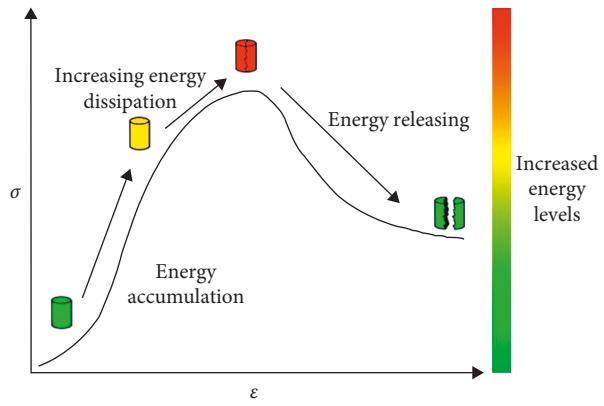

Figure 6: Evolution of containing energy level.

storage limit. To describe the evolution of energy allocation, the ratio of elastic strain energy density to input energy density is defined as storage energy ratio, which is used to characterize the elastic energy storage features under different stress levels. The ratio of dissipation energy density to the input energy density is defined as dissipation energy ratio, which is used to characterize energy consumption and reflect the change in internal structure under different stress levels. The ratio of dissipation energy density to elastic energy density is defined as energy allocation ratio. Input energy density, elastic strain energy density, dissipation energy density, and storage energy ratio were obtained from stress-strain curves under different confining pressures, as shown in Figure 7.

As shown in Figure 7, the energy density increased nonlinearly with strain and increased slowly at the initial loading stage and then entered into the linear development stage, which corresponded to the compression stage and elastic deformation stage. The elastic energy density and input energy density almost coincided at the low stress level, which indicated that stored energy played an important role at this stage. When samples entered the unsteady fracture propagation stage, input energy density continued to improve and the trend of increase in elastic energy density became slow. However, increase in dissipation energy density was accelerated at the same time. This is because the local structure was adjusted under a high stress level, and the development and penetration of internal cracks consumed more energy. The elastic energy density slowed down with the adjustment of the internal structure, but its value was much larger than the dissipation energy density. The storage energy ratio presented an inverted "U"-shaped relationship with strain. The closure of initial cracks and non-reopening of some cracks after unloading were the main reasons for the increase in storage energy ratio. Energy was in the dynamic equilibrium of continuous storage and release in the elastic stage, so storage energy ratio was fairly stable. The dramatic change of internal structure led to the decrease of energy storage capacity and increase of dissipation capacity with an increase in deformation. More transgranular damage occurred within internal structure due to crack propagation and penetration, causing the storage energy ratio to drop sharply. When the input energy exceeded energy storage limit, drastic release of stored energy in rock led to dynamic failure.

The quantitative relationship between elastic energy density and relative stress level was represented by an exponential function (Figure 8). The elastic energy density under large confining pressure was greater than that under low confining pressure at the same stress level, and the growth gradient improved gradually. Stiffness and the energy storage level of rock were positively correlated with confining pressure. The variation in storage energy limit with confining pressure is shown in Figure 9. Maximum storage energy density was 0.28 $MJ \cdot m^{-3}$, 0.55 $MJ \cdot m^{-3}$, 0.78 $MJ \cdot m^{-3}$, 1.13 $MJ \cdot m^{-3}$, 1.77 $MJ \cdot m^{-3}$, and 2.05 $MJ \cdot m^{-3}$, respectively, under six different confining pressures, which were 1.96, 2.79, 4.04, 6.32, and 7.32 times of 1 MPa confining pressure. The maximum storage energy density also represented a trend of exponential growth with confining pressure.

The variation in storage energy ratio with strain under six different confining pressures was plotted as shown in Figure 10. The maximum storage energy ratio was 91.6%, 93.5%, 94.8%, 95.0%, 95.6%, and 96.6%, respectively, for six confining pressures. It showed that the increase of confining pressure not only increased the intensity of input energy but also improved the efficiency of energy accumulation. If loading was suddenly relieved in one direction at a high stress level, rock would release abundant elastic energy and induce rock burst or other dynamic disasters. Rock continued to reserve elastic energy due to internal structural adjustment during the postpeak stage and even resulted in a secondary sharp stress release.

3.4. Dissipation Energy. The stress-strain curve subjected to loading-unloading cycles manifested obvious strain hysteresis, and hysteresis loop area could be used to reflect development of dissipation energy. Hysteresis loop area in the compaction and elasticity stage grew slowly within the strain range of 0–0.2%. The effect of confining pressure on dissipation energy was insignificant (Figure 11). Hysteresis loop area grew linearly within the strain range of 0.2%–0.3% and nonlinearly within the strain range of 0.3% peak strain. Under different confining pressures, the quantitative relationship between the hysteresis loop area and strain was indicated by a quadratic function. The development of dissipation energy was the result of accumulated damage, which further explained the process of crack evolution from closure to initiation, propagation, and finally to failure.

The energy consumption ratio varied in the range of 0.05–0.14 and manifested a U-shaped distribution as shown in Figure 12, which corresponded to the growth pattern of the hysteresis loop area. In fact, there was a one-to-one correspondence between rock strength and energy evolution. Accumulated energy played a more important role compared to the dissipation energy before failure. However, when dissipation energy or damage reached their threshold, the elastic energy would be released sharply along the main fracture surface, and the friction between fracture surfaces consumed more energy. Therefore, the catastrophe point of

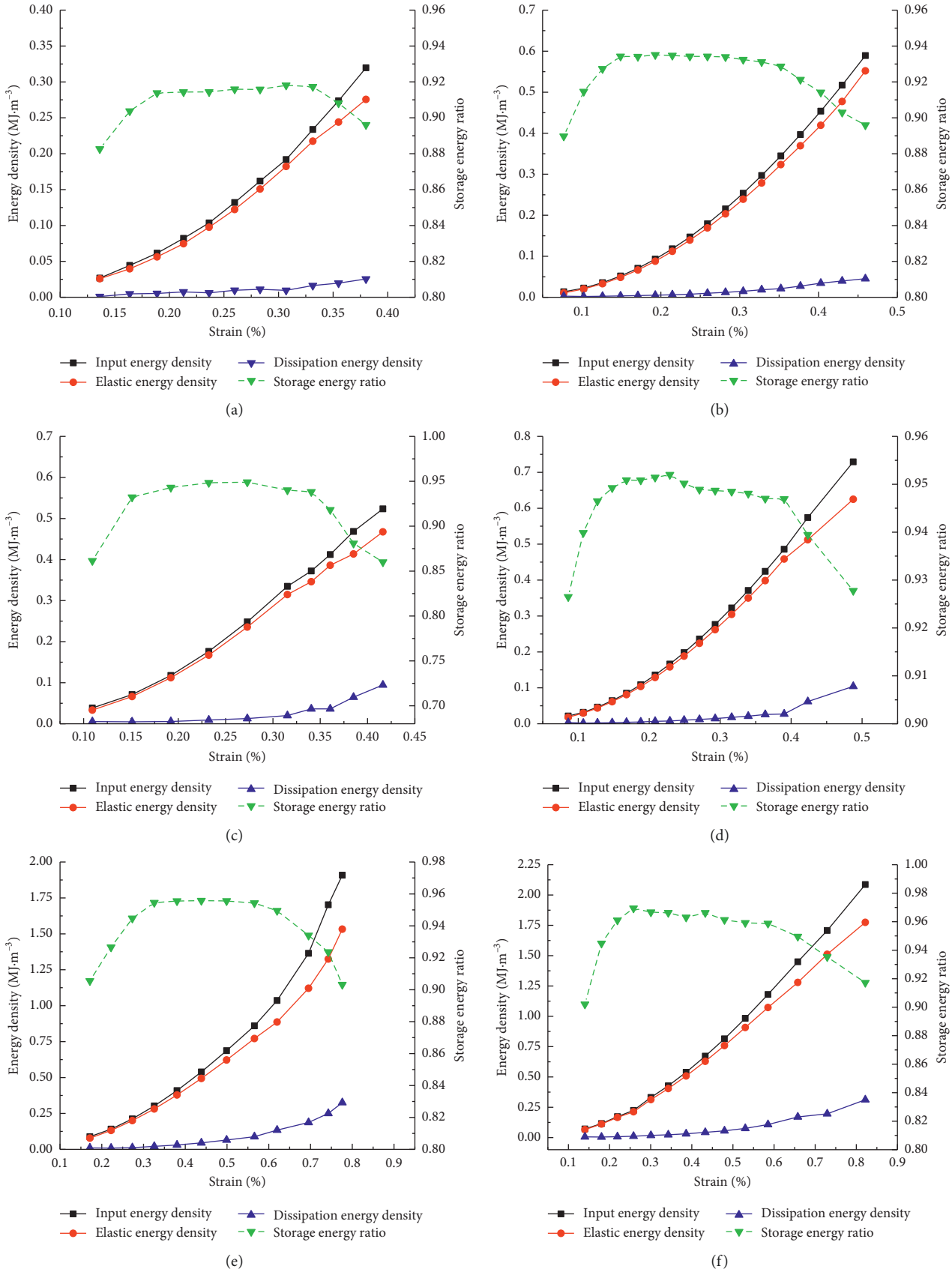

Figure 7: Energy evolution under six different confining pressures. (a) 1 MPa. (b) 10 MPa. (c) 20 MPa. (d) 30 MPa. (e) 40 MPa. (f) 45 MPa.

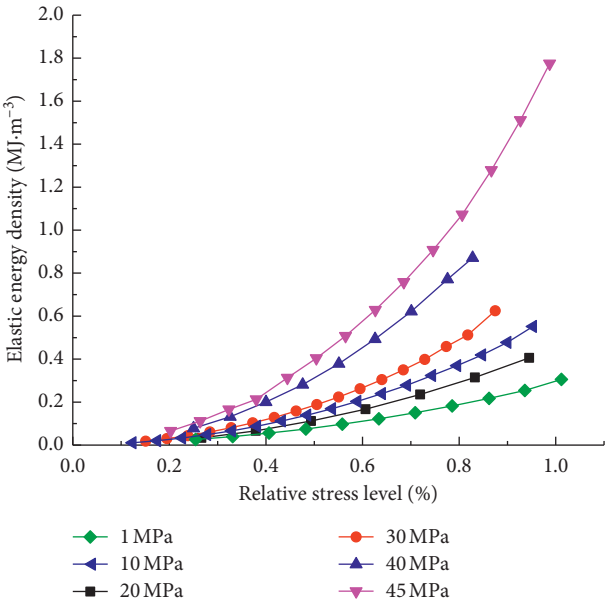

Figure 8: Elastic energy density with relative stress level.

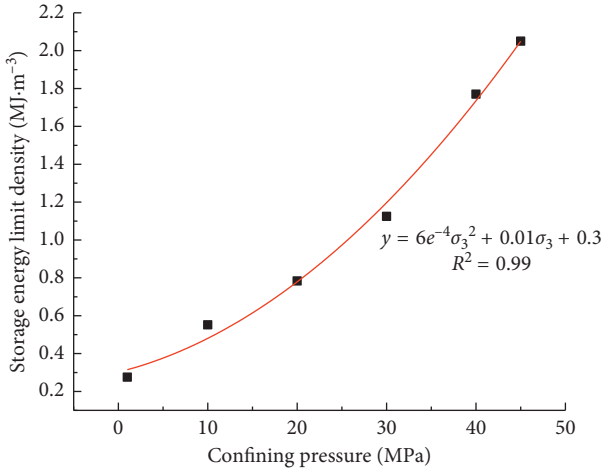

Figure 9: Energy limit density with confining pressure.

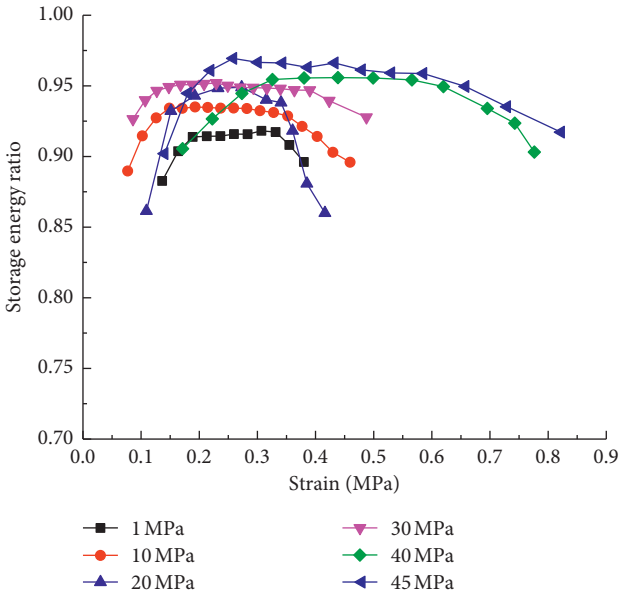

Figure 10: Storage energy ratio with strain.

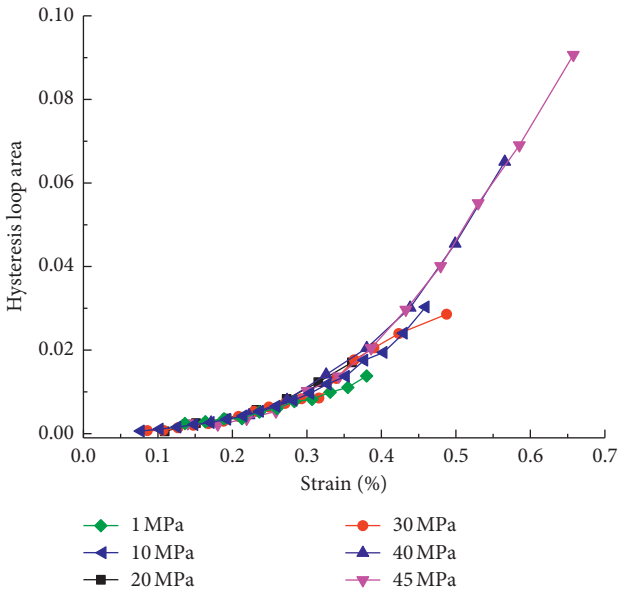

Figure 11: Variation of hysteresis loop area.

energy consumption ratio can be used as a precursor information for failure.

Dilatancy is a general inelastic volume deformation phenomenon of rock and is a result of unstable development of cracks. The dilatancy point is the turning point of volume changing from compression to expansion and indicates that rock is about to enter the fracture instability development stage. Dilatancy is inevitably related to dissipation energy, and the dilatancy point can be used as the starting point for the unstable development of internal cracks. Dilatancy stress in this experimental study was about 68%–83% of the peak stress level under different confining pressures shown in Table 2. Samples under 1 MPa confining pressure were taken only as an example for analysis, and the results of other samples were similar. Figure 13 shows that evolution of dissipation energy with strain can be divided into four distinct stages, namely, rapidly increasing, slowly increasing, accelerated increasing, and sharply increasing. As the separation point between the second and third stage, the dissipation energy increased slowly before the dilatancy point but accelerated after the dilatancy point. Therefore, the dilatancy point can be used as a catastrophe point of dissipation energy and a precursor for failure.

3.5. Correlation between Mechanical Parameters and Energy Evolution. Internal structure is constantly adjusted so that the mechanical parameters change significantly under cyclic loading and unloading. The internal structure determines energy evolution, and hence, establishment of a relationship between mechanical parameters and energy evolution is useful to predict rock failure. The correlation between elastic

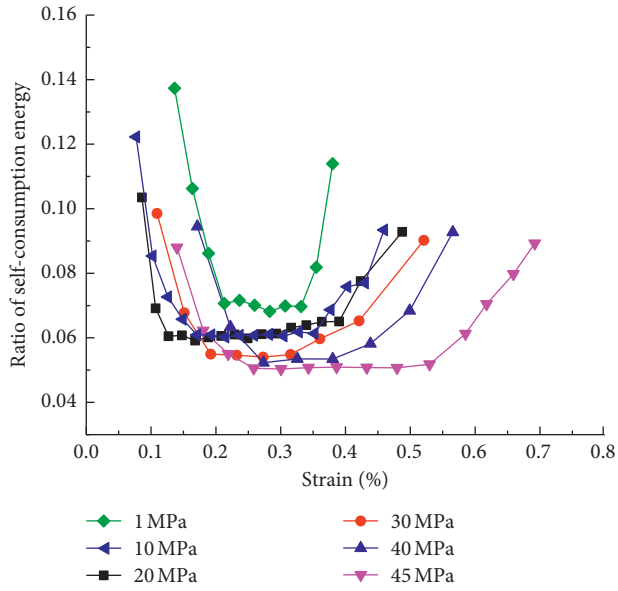

Figure 12: Variation of energy consumption.

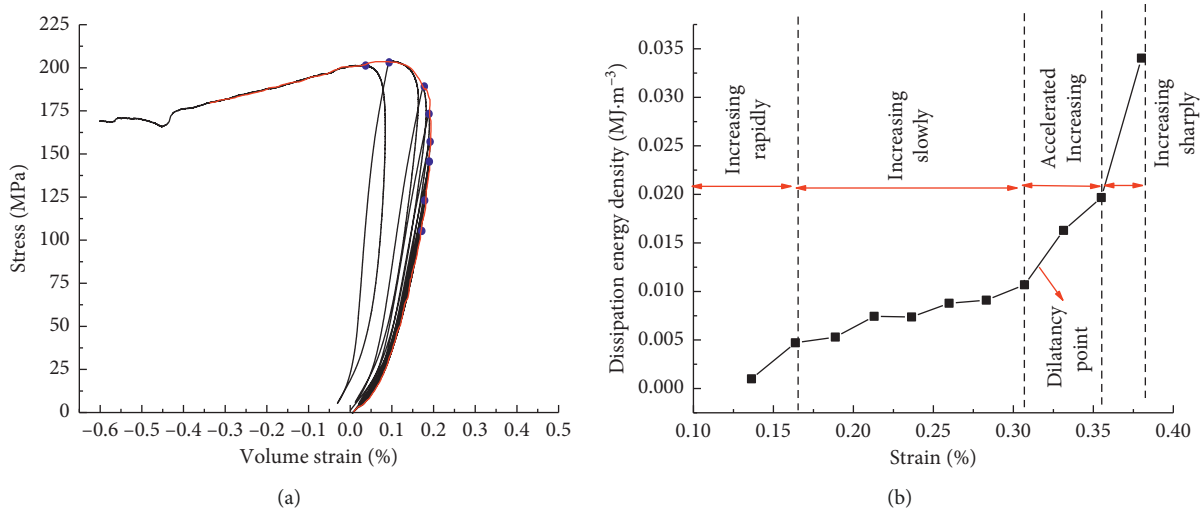

Figure 13: Variation in volumetric strain and dissipative energy under 1 MPa confining pressure. (a) Outer envelope of volume strain. (b) Variation in dissipation energy with strain.

modulus, Poisson's ratio, loading/unloading response ratio, and energy evolution were analysed. Elastic modulus [17] was obtained by linear fitting of stress-strain data during loading and unloading, and Poisson's ratio was calculated according to the linear stress-strain data. Loading/unloading response ratio was a state parameter of a nonlinear system, and it could provide an important information for predicting instability. Loading/unloading response ratio [18]is defined as

$$Y = \frac{X_+}{X_-} = \frac{1/E_+}{1/E_-} = \frac{E_-}{E_+}, \quad (2)$$

where X_- and X_+ are the strain responses of unloading and loading, respectively, E_- and E_+ are the elastic modulus of unloading and loading, respectively.

Elastic modulus and Poisson's ratio are the direct reflection of rock stiffness which is an ability index to resist elastic deformation. The limit of storage energy is mainly decided by rock stiffness. Elasticity modulus with loading/unloading cycles revealed an inverted "U" shape (Figure 14); that is, the variation in elastic modulus increased first, then became stable for some time, and decreased finally. Compression of original fissures in the compaction stage improved rock compactness and elastic modulus, and the storage energy ratio increased slightly from an energy perspective. The elastic modulus fluctuated within a certain range due to the relatively less damage in the elastic stage. The initiation and propagation of cracks in the unsteady development stage resulted in an increase in internal structural damage, a decline in elastic modulus, and overall stiffness.

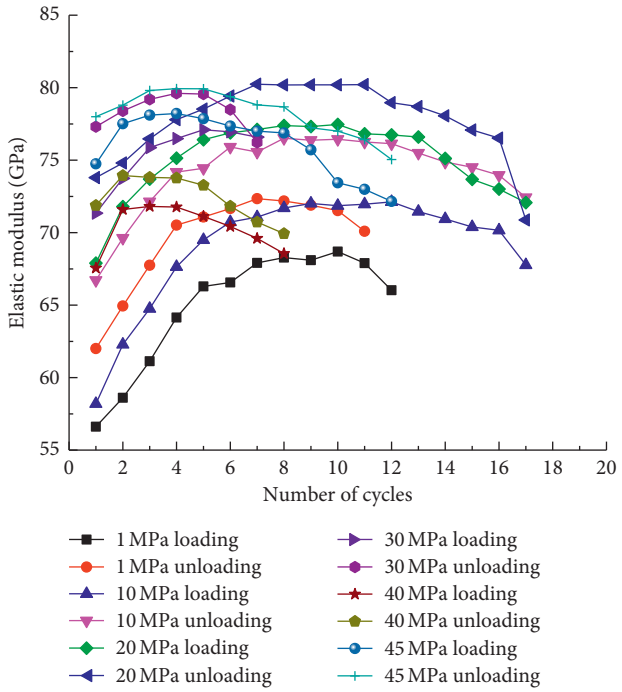

Figure 14: Variation of elastic modulus with cycles.

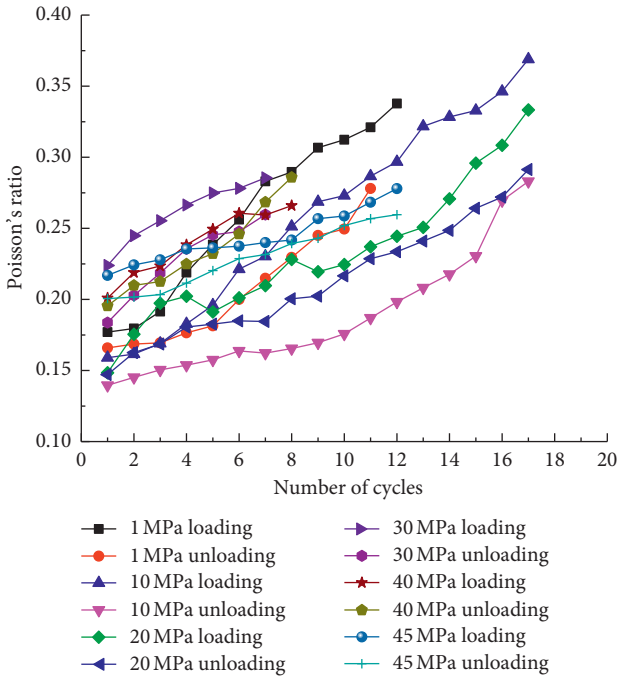

Figure 15: Variation of Poisson's ratio with cycles.

Poisson's ratio during loading/unloading cycles was within the range of 0.15~0.33 and increased nonlinearly with the number of cycles as shown in Figure 15. Poisson's ratio in the loading stage was always greater than in the unloading stage. For an analysis, the value of Poisson's ratio was taken corresponding to an unloading cycle.

The increase in Poisson's ratio indicated the deterioration of internal structure and the enhancement of transverse deformation. Poisson's ratio was influenced by confining pressure effect during the whole process of rock deformation and failure, and transverse deformation was restricted with an increase in confining pressure as shown in Table 3. The input energy could not be fully consumed and was stored in rock mass in the form of strain energy, thus continuously increasing the energy storage level. The direct reason of rock mass instability is that accumulated energy in rock mass exceeded the bearing capacity of the rock mass.

The loading/unloading response ratio decreased first, then stabilized subsequently, and decreased finally. It was generally greater than one under six different confining pressures, thus indicating that elastic modulus in the unloading stage is always greater than in the loading stage (Figure 16). Both E_- and E_+ increased with the number of cycles under the low stress level. However, due to the reopening of some cracks in the unloading stage, the level of increase during unloading was smaller compared to that during loading. The loading and unloading elastic modulus remained fairly stable in the elastic stage, and the response ratio fluctuated within a certain range.

Elastic modulus decreased faster in the unloading stage than in the loading stage. The loading/unloading response ratio decreased rapidly. Therefore, the change in loading/

Table 3: Poisson's ratio of whole loading process.

Confining pressure (MPa)	Initial Poisson's ratio	Failure Poisson's ratio	Increment	Rate of increase (%)
1	0.15	0.3	0.15	100
10	0.14	0.28	0.14	100
20	0.15	0.29	0.14	93
30	0.18	0.26	0.08	44
40	0.20	0.27	0.07	35
45	0.20	0.26	0.06	30

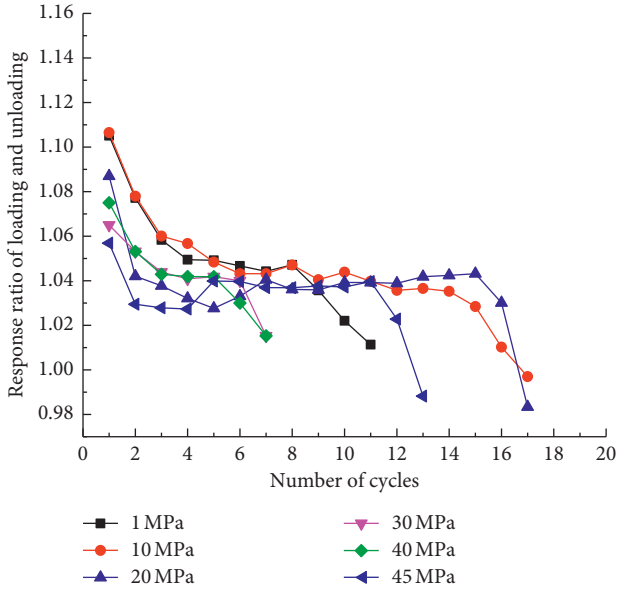

Figure 16: Variation of loading/unloading response ratio.

unloading response ratio from the stable stage to the stage of secondary decrease can provide an important precursor information for unsteady fracture development. The accumulated damage caused by internal structural adjustment resulted in the decrease of elastic modulus and the increase of Poisson's ratio, especially entering into the fracture instability development stage. Test results showed that there was a positive correlation between energy storage limit and elastic modulus but a negative correlation between Poisson's ratio and energy dissipation.

4. Conclusion

Confining pressure effects on variation and allocation of energy were revealed based on the triaxial cyclic loading and unloading testing of granite under six different confining pressures. The correlation between mechanical parameters variation and energy characteristics was also discussed.

(1) The outer envelope of stress-strain curves under six different confining pressures is similar to conventional loading. The failure modes developed from a well-developed surface fracture to a single through fracture. Allocation of energy was determined by internal structure, and the containing energy level of rock depends on the stress level.

(2) Elastic energy density was always greater than dissipation energy density, indicating that accumulated energy was dominant before the peak stress. Storage energy limit improved nonlinearly with the confining pressure, and the energy consumption ratio showed an inverted U shape with strain. The hysteresis loop area had an obvious quadratic relationship with strain.

(3) As the confining pressure increased, the elastic energy density increased nonlinearly at the same stress level and the growth gradient also improved gradually at the same time. High confining pressure improved the stiffness of rock and increased the energy storage level. Elastic modulus and energy consumption ratio presented an inverted "U" type and a "U" type, respectively, which confirmed good correlation between mechanical parameters and energy evolution characteristics.

(4) Elastic modulus and Poisson's ratio are characteristics of rock stiffness. Larger elastic modulus and smaller Poisson's ratio indicate that rock stiffness and storage energy limit are greater. The characteristic of loading/unloading response ratio from the stable stage to secondary decrease could be regarded as the precursor information of unsteady fracture development.

(5) There were four distinct stages in the curve of dissipation energy with strain. The dilatancy point was the key point after which dissipation energy was accelerated. The dilatancy point could provide an important information for the unsteady development of fracture.

Data Availability

The data used to support the findings of this study are available from the corresponding author upon request.

Conflicts of Interest

The authors declare that there are no conflicts of interest regarding the publication of this paper.

Acknowledgments

This paper was supported by Project no. 2016YFC0600801 of the National Key Research and Development Plan and Key Program of National Natural Science Foundation of China (51534002). The financial aids are gratefully acknowledged.

References

[1] T. W. Liu, J. D. He, and J. W. Xu, "Energy properties of failure of marble samples under triaxial compression," *Chinese Journal of Geotechnical Engineering*, vol. 35, no. 2, pp. 395–400, 2013.

[2] C. S. Wang, H. W. Zhou, Z. H. Wang et al., "Investigation on the rockburst proneness of Beishan granite under different stress state," *Advanced Engineering Sciences*, vol. 49, no. 6, pp. 84–90, 2017.

[3] L. T. Xie, P. Yan, W. B. Lu et al., "Energy accumulation properties of deep rock under different excavation methods," *Journal of Huazhong University of Science and Technology (Natural Science Edition)*, vol. 46, no. 1, pp. 120–125, 2018.

[4] J. W. Liu, B. X. Huang, and M. T. Wei, "Influence of cyclic uniaxial loading on coal elastic-plastic properties and energy accumulation and dissipation," *Journal of Liaoning Technical University: Natural Science*, vol. 31, no. 1, pp. 26–30, 2012.

[5] Y. Li, S. Zhang, and X. Zhang, "Classification and fractal characteristics of coal rock fragments under uniaxial cyclic loading conditions," *Arabian Journal of Geosciences*, vol. 11, no. 9, p. 201, 2018.

[6] M. F. Cai, G. Y. Kong, and L. H. Jia, "Criterion of energy catastrophe for rock project system failure in underground engineering," *Journal of University of Science and Technology Beijing*, vol. 19, no. 4, pp. 325–328, 1997.

[7] G. L. Wang, L. Zhang, Xu M. et al., "Research on energy damage evolution mechanism of non-across jointed rock mass under uniaxial compression," *Chinese Journal of Geotechnical Engineering*, vol. 46, no. 8, pp. 1–9, 2018.

[8] R. D. Peng, Y. Ju, F. Gao et al., "Energy analysis on damage of coal under cyclical triaxial loading and unloading conditions," *Journal of China Coal Society*, vol. 39, no. 2, pp. 245–252, 2014.

[9] Z. Z. Zhang and F. Gao, "Research on nonlinear characteristics of rock energy evolution under uniaxial compression," *Chinese Journal of Rock Mechanics and Engineering*, vol. 31, no. 6, pp. 1198–1207, 2012.

[10] Z. Z. Zhang and F. Gao, "Confining pressure effect on rock energy," *Chinese Journal of Rock Mechanics and Engineering*, vol. 34, no. 1, pp. 1–11, 2015.

[11] J. Cheng, J. T. Zhang, J. J. Han et al., "Research status of energy dissipation of rock under different stress paths and analysis," *China Mining Magazine*, vol. 27, no. 1, pp. 148–153, 2018.

[12] M. N. Bagde and V. Petroš, "Fatigue and dynamic energy behaviour of rock subjected to cyclical loading," *International*

Journal of Rock Mechanics and Mining Sciences, vol. 46, no. 1, pp. 200–209, 2009.

[13] H. F. Deng, Y. Y. Hu, and J. L. Li, "Experimental research on the load/unload response ratio considering the hysteresis effect of rock," *Chinese Journal of Rock Mechanics and Engineering*, vol. 34, no. 1, pp. 2915–2921, 2015.

[14] H. F. Deng, Y. Hu, and J. L. Li, "The evolution of sandstone energy dissipation under cyclic loading and unloading," *Chinese Journal of Rock Mechanics and Engineering*, vol. 35, no. 1, pp. 2869–2875, 2016.

[15] Y. Tian and R. G. Yu, "Energy analysis of limestone during triaxial compression under different confining pressures," *Rock and Soil Mechanics*, vol. 35, no. 1, pp. 118–129, 2014.

[16] F. Q. Huang, Y. Li, Z. H. Dou et al., "Analysis on deformation failure and energy properties of granite under triaxial compression in Xi'anshan iron mine," *Mining R&D*, vol. 36, no. 7, pp. 82–85, 2016.

[17] G. C. Jia, J. H. Chen, Y. T. Yin et al., "Research on mechanical behaviors and failure modes of layer shale," *Rock and Soil Mechanics*, vol. 34, no. 2, pp. 57–61, 2013.

[18] Z. R. Tu and Q. Yang, "Test research on negative Poisson's ratio of rock mass," *Rock and Soil Mechanics*, vol. 29, no. 10, pp. 2833–2836, 2008.